Quantum state measurement in double quantum dots with a radio-frequency quantum point contact*

Yan Lei(严 蕾), Wang Hai-Xia(王海霞), Yin Wen(殷 雯)†, and Wang Fang-Wei(王芳卫)

Institute of Physics, Chinese Academy of Sciences, Beijing 100190, *China*

(Received 13 August 2013; revised manuscript received 12 September 2013; published online 10 December 2013)

We study the dynamics of two electron spins in coupled quantum dots (CQDs) monitored by a quantum point contact (QPC) detector. Their quantum state can be measured by embedding the QPC in an LC circuit. We derive the Bloch-type rate equations of the reduced density matrix for CQDs. Special attention is paid to the numerical results for the weak measurement condintion under a strong Coulomb interaction. It is shown that the evolution of QPC current always follows that of electron occupation in the right dot. In addition, we find that the output voltage of the circuit can reflect the evolution of QPC current when the circuit and QPC are approximately equal in frequency. In particular, the wave shape of the output voltage can be improved by adjusting the circuit resonance frequency and bandwidth.

Keywords: measurement, quantum state, output voltage, circuit parameter

PACS: 03.65.Yz, 03.67.Lx, 73.23.Hk **DOI:** 10.1088/1674-1056/23/2/020305

1. Introduction

Semiconductor technology is rapidly approaching a level such that quantum systems comprising one or two electron spins can be confined or manipulated within a nanostructure device.[1–3] These improvements accelerate new applications in quantum computational schemes. Obviously, a key factor for the quantum computational scheme is reading out the quantum spin states, thus, the methods of measuring quantum states are still being investigated extensively, both theoretically and experimentally.[4–10] Quantum point contact (QPC) and single electron transistor (SET) have been used to continuously measure a charge quantum bit (qubit), which is the superposition of two basic quantum states $|\Psi_0\rangle = \cos\alpha\,|1\rangle + \mathrm{e}^{\mathrm{i}r}\sin\alpha\,|2\rangle$ with two real parameters α and γ.[11] In one realization of a solid-state based qubit, the two basic states represent a single-level quantum dot.[8] The Hamiltonian is given by $H = E_1 a_1^{\dagger} a_1 + E_2 a_2^{\dagger} a_2 + \Omega a_1^{\dagger} a_2 + \mathrm{H.c.}$ Provided that the QPC is close to the quantum dot, the QPC current drops due to the electrostatic repulsion between electrons. It is clear that one can use a QPC as a sensitive detector for measuring qubits.

Recently, the readout of a few-electron double quantum dot with fast radio-frequency (rf) gate-sensors was realized experimentally.[12] In addition, Wang *et al.* studied the thermoelectric transport through a double-quantum-dot system with spin-dependent interdot coupling.[13] Furthermore, Oxtoby *et al.*[14] theoretically introduced the so-called radio-frequency quantum point contact (rf-QPC) for monitoring charge qubits. The principle of the rf-QPC operation is somewhat similar to the operation of radio-frequency superconducting quantum interference devices[15] and is based on the microwave reflection from a tank circuit that consists of an inductor L and a capacitor C. In this scheme, embedding the QPC provides the tank circuit a damping source, so the oscillator damping depends on the qubit state via the qubit-dependent QPC current.

In this paper, we discuss an alternative theoretical scheme whereby the spin state of two coupled quantum dots (CQDs) can be inferred by observing the nearby QPC current. Spin-dependent charge current can be observed by continuously measuring two CQDs with a QPC adjacent to one of the dots (see Fig. 1). QPC is used as an electrometer in this work, although it might equivalently be a SET or a double dot (DD) detector.[8] Note that the QPC here acts both as a noise source that can induce inelastic transitions in the quantum dots and as a detector to observe these transitions. According to the Pauli Exclusion Principle, two electrons with different spins may occupy one dot at most. The electron may oscillate between two dots with its spin not flipping. Based on the method proposed by Gurvitz *et al.*,[16,17] we first derive the Bloch-type rate equations of the system. Then, we investigate the relationship between the spin state of the dots and the QPC current numerically. It is found that the spin state can be directly extracted from the measured QPC current. We use these results to simulate individual runs of the measurement scheme and to characterize the output for the different measurement conditions. To read out the spin state, we then embed the above quantum system in an LC circuit, just as Oxtoby *et al.*,[14] did. We conclude by briefly discussing how this technique could be used to measure spin states and also to improve the output voltage signal.

*Project supported by the National Natural Science Foundation of China (Grant No. 11174358) and the National Basic Research Program of China (Grant No. 2010CB833102).

†Corresponding author. E-mail: wenyin@aphy.iphy.ac.cn

© 2014 Chinese Physical Society and IOP Publishing Ltd

2. Model and formulation

The CQDs system, including a QPC detector, is schematically shown in Fig. 1. We represent the QPC as a tunnel barrier between source and drain leads (reservoirs) with respective Fermi levels $\mu_{\rm L}$ and $\mu_{\rm R}$. The two-electron coupled-dot system can be described by the Hamiltonian

$$H = H_{\rm CQD} + H_{\rm QPC} + H_{\rm int}. \tag{1}$$

The Hamiltonian for CQDs is

$$\begin{aligned} H_{\rm CQD} &= \sum_{i,\sigma} E_i a^{\dagger}_{i,\sigma} a_{i,\sigma} + \sum_{\sigma} \Omega_0 (a^{\dagger}_{1\sigma} a_{2\sigma} + a^{\dagger}_{2\sigma} a_{1\sigma}) \\ &\quad + U_1 \sum_i n_{i\uparrow} n_{i\downarrow} + U_2 \sum_{\sigma,\sigma'} n_{1\sigma} n_{2\sigma'}, \end{aligned} \tag{2}$$

where the subscript $i = 1,2$ indicates the left or right quantum dot, $a^{\dagger}_{i\sigma}$ ($a_{i\sigma}$) is the creation (annihilation) operator of the electron with spin σ ($\sigma = \uparrow, \downarrow$) in the i-th quantum dot, E_i is the energy level of the i-th quantum dot, Ω_0 is the tunnel-coupling amplitude, $n_{i\sigma} = a^{\dagger}_{i\sigma} a_{i\sigma}$ is the occupation number operator of the i-th quantum dot, U_1 is the intradot Coulomb repulsion energy and U_2 is the interdot Coulomb repulsion energy. The Hamiltonian for QPC is

$$H_{\rm QPC} = \sum_l E_l c^{\dagger}_l c_l + \sum_r E_r c^{\dagger}_r c_r + \sum_{l,r} \Omega_{lr} (c^{\dagger}_r c_l + c^{\dagger}_l c_r), \tag{3}$$

where the operators $c^{\dagger}_l$ (c_l) and $c^{\dagger}_r$ (c_r) correspond to the creation (annihilation) of an electron for the left and right reservoirs, respectively. $H_{\rm int}$ describes the electrostatic interaction between QPC and CQDs,

$$\begin{aligned} H_{\rm int} &= \sum_{l,r} \delta\Omega_{lr} a^{\dagger}_{1\uparrow} a_{1\uparrow} (c^{\dagger}_r c_1 + c^{\dagger}_l c_r) \\ &\quad + \sum_{l,r} \delta\Omega_{lr} a^{\dagger}_{1\downarrow} a_{1\downarrow} (c^{\dagger}_r c_l + c^{\dagger}_l c_r), \end{aligned} \tag{4}$$

where $\delta\Omega_{lr}$ is the change in the effective QPC tunnelling amplitude Ω_{lr} when the nearby dot is occupied and is independent of the electron spin state. The so-called vacuum state $|0\rangle$ corresponds to the levels in the reservoirs being filled up to the Fermi energies and the CQDs being kept empty. Without loss of generality, we assume that two opposite-spin electrons occupy the left dot of the CQDs initially. The evolution of the whole system is described by the wave function as

$$\begin{aligned} |\Psi(t)\rangle &= [b_1(t) a^{\dagger}_{1\uparrow} a^{\dagger}_{1\downarrow} + b_2(t) a^{\dagger}_{1\uparrow} a^{\dagger}_{2\downarrow} \\ &\quad + b_3(t) a^{\dagger}_{1\downarrow} a^{\dagger}_{2\uparrow} + b_4(t) a^{\dagger}_{2\uparrow} a^{\dagger}_{2\downarrow} \\ &\quad + \sum_{l,r} b_{1lr}(t) a^{\dagger}_{1\uparrow} a^{\dagger}_{1\downarrow} c^{\dagger}_r c_l + \sum_{l,r} b_{2lr}(t) a^{\dagger}_{1\uparrow} a^{\dagger}_{2\downarrow} c^{\dagger}_r c_l \\ &\quad + \sum_{l,r} b_{3lr}(t) a^{\dagger}_{1\downarrow} a^{\dagger}_{2\uparrow} c^{\dagger}_r c_l \\ &\quad + \sum_{l,r} b_{4lr}(t) a^{+}_{2\uparrow} a^{\dagger}_{2\downarrow} c^{\dagger}_r c_l + \cdots] |0\rangle, \end{aligned} \tag{5}$$

where $b_k(t)$, $k = 1,2,3,4,1lr,2lr,\ldots$ are the time-dependent probability amplitudes for finding the system in the corresponding states described above with the initial condition $b_1(0) = 1$ and all the other $b(0) = 0$.

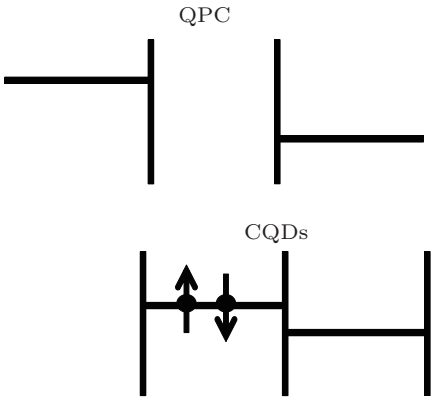


Fig. 1. Schematic illustration of the spin state readout scheme.

We now introduce the density matrix of the system. According to the electron occupancy of the CQDs (see Fig. 2), the system has four possible states, namely: $|1\rangle$ represents two electrons with different spins in the left dot, $|2\rangle$ represents one electron with spin up in the left dot and the other electron with spin down in the right dot, $|3\rangle$ represents one electron with spin down in the left dot and the other electron with spin up in the right dot, and $|4\rangle$ represents two electrons with different spins in the right dot.

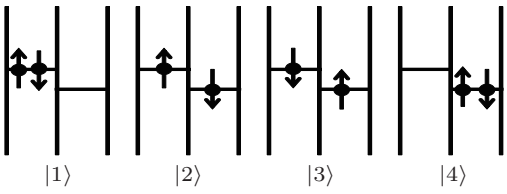


Fig. 2. All possible electron states of the CQDs.

In the four-dimensional Fock space composed of $|1\rangle$, $|2\rangle$, $|3\rangle$, and $|4\rangle$, using the method Gurvitz *et al.*[16] developed, we can derive the following set of equations for the density matrix elements of the system:

$$\dot{\sigma}_{11} = {\rm i}\Omega_0(\sigma_{12} - \sigma_{21}) + {\rm i}\Omega_0(\sigma_{13} - \sigma_{31}), \tag{6a}$$

$$\dot{\sigma}_{22} = {\rm i}\Omega_0(\sigma_{21} - \sigma_{12}) + {\rm i}\Omega_0(\sigma_{24} - \sigma_{42}), \tag{6b}$$

$$\dot{\sigma}_{33} = {\rm i}\Omega_0(\sigma_{31} - \sigma_{13}) + {\rm i}\Omega_0(\sigma_{34} - \sigma_{43}), \tag{6c}$$

$$\dot{\sigma}_{44} = {\rm i}\Omega_0(\sigma_{42} - \sigma_{24}) + {\rm i}\Omega_0(\sigma_{43} - \sigma_{34}), \tag{6d}$$

$$\begin{aligned} \dot{\sigma}_{12} &= {\rm i}\Omega_0(\sigma_{11} - \sigma_{22}) + {\rm i}\Omega_0(\sigma_{14} - \sigma_{32}) \\ &\quad + \sqrt{D'D''}\sigma_{12} + {\rm i}(E_2 - E_1)\sigma_{12} + {\rm i}(U_2 - U_1)\sigma_{12} \\ &\quad - \frac{1}{2}(D' + D'')\sigma_{12}, \end{aligned} \tag{6e}$$

$$\begin{aligned} \dot{\sigma}_{13} &= {\rm i}\Omega_0(\sigma_{11} - \sigma_{33}) + {\rm i}\Omega_0(\sigma_{14} - \sigma_{23}) \\ &\quad + \sqrt{D'D''}\sigma_{13} + {\rm i}(E_2 - E_1)\sigma_{13} + {\rm i}(U_2 - U_1)\sigma_{13} \\ &\quad - \frac{1}{2}(D' + D'')\sigma_{13}, \end{aligned} \tag{6f}$$

$$\begin{aligned} \dot{\sigma}_{14} &= {\rm i}\Omega_0(\sigma_{13} - \sigma_{34}) + {\rm i}\Omega_0(\sigma_{12} - \sigma_{24}) \\ &\quad + \sqrt{DD''}\sigma_{14} + 2{\rm i}(E_2 - E_1)\sigma_{14} \end{aligned}$$

$$-\frac{1}{2}(D+D'')\sigma_{14}, \tag{6g}$$

$$\dot{\sigma}_{23} = \mathrm{i}\Omega_0(\sigma_{21}-\sigma_{13})+\mathrm{i}\Omega_0(\sigma_{24}-\sigma_{43}), \tag{6h}$$

$$\begin{aligned}\dot{\sigma}_{24} = {} & \mathrm{i}\Omega_0(\sigma_{22}-\sigma_{44})+\mathrm{i}\Omega_0(\sigma_{23}-\sigma_{14})\\ & +\sqrt{D'D}\sigma_{24}+\mathrm{i}(E_2-E_1)\sigma_{24}+\mathrm{i}(U_1-U_2)\sigma_{24}\\ & -\frac{1}{2}(D'+D)\sigma_{24},\end{aligned} \tag{6i}$$

$$\begin{aligned}\dot{\sigma}_{34} = {} & \mathrm{i}\Omega_0(\sigma_{32}-\sigma_{14})+\mathrm{i}\Omega_0(\sigma_{33}-\sigma_{44})\\ & +\sqrt{D'D}\sigma_{34}+\mathrm{i}(E_2-E_1)\sigma_{34}+\mathrm{i}(U_1-U_2)\sigma_{34}\\ & -\frac{1}{2}(D'+D)\sigma_{34},\end{aligned} \tag{6j}$$

where $D = 2\pi\rho_{\mathrm{L}}\rho_{\mathrm{R}}\Omega_{lr}^2(\mu_{\mathrm{L}}-\mu_{\mathrm{R}})$, $D' = 2\pi\rho_{\mathrm{L}}\rho_{\mathrm{R}}(\Omega_{lr}+\delta\Omega_{lr})^2(\mu_{\mathrm{L}}-\mu_{\mathrm{R}})$, and $D'' = 2\pi\rho_{\mathrm{L}}\rho_{\mathrm{R}}(\Omega_{lr}+2\delta\Omega_{lr})^2(\mu_{\mathrm{L}}-\mu_{\mathrm{R}})$ represent the corresponding tunnelling rate from the left lead to the right lead of the QPC when zero, one or two electrons stay in the left quantum dot, respectively. $\rho_{\mathrm{L(R)}}$ is the density of states in the left (right) lead, since the states in the leads are very dense (continuum).

According to the general current formula,[16,17] the current flowing through the QPC can be given by

$$I(t) = e[D''\sigma_{11}+D'(\sigma_{22}+\sigma_{33})+D\sigma_{44}]. \tag{7}$$

3. Measurement circuit

Now, we embed this QPC and CQDs system in the radio-frequency circuit. This procedure was proposed by Oxtoby *et al.*[14] This circuit is a classical oscillator consisting of an inductor L and a capacitor C. Embedding a dissipative component QPC into the circuit will produce a source of damping. In this case, the damping depends on the QPC current and, therefore, depends on the spin states of the electrons.

The total current coming from the QPC is $\tilde{I}(t) = e|T|J(t)+I_{\mathrm{clas}}(t)$, where $I_{\mathrm{clas}}(t)$ is the classical signal and the remaining part is the quantum signal. We make the approximation $T \approx T_0 = \sqrt{D}$ due to $\varepsilon_{\mathrm{in}} \ll 1$, so we further get the quantum signal $J(t) \approx I(t)/(eT_0)$, where $I(t)$ is given by Eq. (7). By beating the output voltage with a local oscillator, the observer would measure the quadrature voltage to read out two quadrature currents. To be more specific, we skip the sophisticated derivation process and give the output voltage as it would be measured by an ideal observer

$$\begin{aligned}V_{\mathrm{out}}^{\cos}(t) = {} & \pi f Z_{\mathrm{TL}}\frac{1}{\mathrm{d}t}\int_0^t \mathrm{d}s\exp\left[-\frac{Z_{\mathrm{TL}}}{2L}(t-s)\right]\\ & \times\int_{s-\mathrm{d}t}^{s}\mathrm{d}kI(k)[\sin(2\pi fk)\\ & +\frac{1}{4}\varepsilon_{\mathrm{in}}(1-\cos(4\pi fk))],\end{aligned} \tag{8a}$$

$$\begin{aligned}V_{\mathrm{out}}^{\sin}(t) = {} & -\pi f Z_{\mathrm{TL}}\frac{1}{\mathrm{d}t}\int_0^t \mathrm{d}s\exp\left[-\frac{Z_{\mathrm{TL}}}{2L}(t-s)\right]\\ & \times\int_{s-\mathrm{d}t}^{s}\mathrm{d}kI(k)[\cos(2\pi fk)\\ & +\frac{1}{4}\varepsilon_{\mathrm{in}}\sin(4\pi fk)],\end{aligned} \tag{8b}$$

where Z_{TL} is the impedance of the transmission line (typically 50 Ω), $B = 1/\mathrm{d}t$ is the bandwidth, $\omega_0 = 1/\sqrt{LC} = 2\pi f$ is the resonance angular frequency and $\varepsilon_{\mathrm{in}}$ is the dimensionless parameter, which represents the ratio of the rf signal and dc signal. Here, QPC is biased (dc) as well as subjected to a small-amplitude sinusoidal carrier signal (rf); thus, $\varepsilon_{\mathrm{in}} \ll 1$. In the high quality limit, the tank circuit damping is mainly from the detector, which requires $\omega_0 \gg Z_{\mathrm{TL}}/L$.

4. CQDs dynamic with the QPC detector

In order to understand the spin state of the electrons in the CQDs, it is instructive to examine the dynamics of the electrons without the QPC detector. In this discussion, we choose the interdot coupling $\Omega_0 \equiv 1.0$ as the energy unit. The levels are aligned ($\Delta E \equiv E_1 - E_2 = 0$) and the Coulomb interactions U_1 and U_2 satisfy the relationship as $U_1 = \sqrt{2}U_2$. Figure 3 shows the occupations of the electrons with the different Coulomb interactions. We find in the case of strong Coulomb interaction (e.g. $U_1 = 80$), the periodical oscillation is kept for both σ_{11} and σ_{44}, which means the strong interdot Coulomb interactions prevent the electrons from occupying the neighboring dots. It is interesting that the electrons staying only in states $|1\rangle$ and $|4\rangle$ will produce the so-called Bell state.[18] Thus, in the following, we focus on the CQDs and QPC system under the condition of the strong Coulomb interaction ($U_1 = \sqrt{2}U_2 = 80$). For convenience, the weak measurement conditions $D' = 0.9D$ and $D'' = 0.9D'$ are considered to minimize the dephasing that reflects the quantum-mechanical cost of obtaining information about the quantum state.

We now discuss the dynamics of electrons with the QPC detector. It can be deduced from Fig. 4(a) that the evolution of QPC current $I(t)$ is consistent with the σ_{44} oscillations. This is easy to comprehend from the physical point of view. When the electrons tunnel into the right dot, the disappearance of the electrostatic repulsion between the CQDs and the QPC minimizes the height of the QPC barrier and, thus, the current reaches its maximum. Figure 4(b) shows the occupation probabilities of the electrons in the left and the right dots. For the stationary state, $\sigma_{11} = \sigma_{44} = 0.5$ in the limit of $t \to \infty$, which comes from the dephasing process due to measurement. Furthermore, we consider the condition that there exists an energy mismatch by tuning the gate voltages of the two dots.[11] Figure 4(c) suggests that when $\Delta E = 0.5\Omega_0$, although the QPC current $I(t)$ still follows σ_{44} closely, it is more difficult to identify the quantum information from the QPC current. In addition, the energy mismatch strongly suppresses coherent oscillations (see Fig. 4(d)). In order to obtain the quantum state information easily, we should limit ourselves to $\Delta E = 0$, which can be adjusted by sweeping across the interdot charge transition.[10]

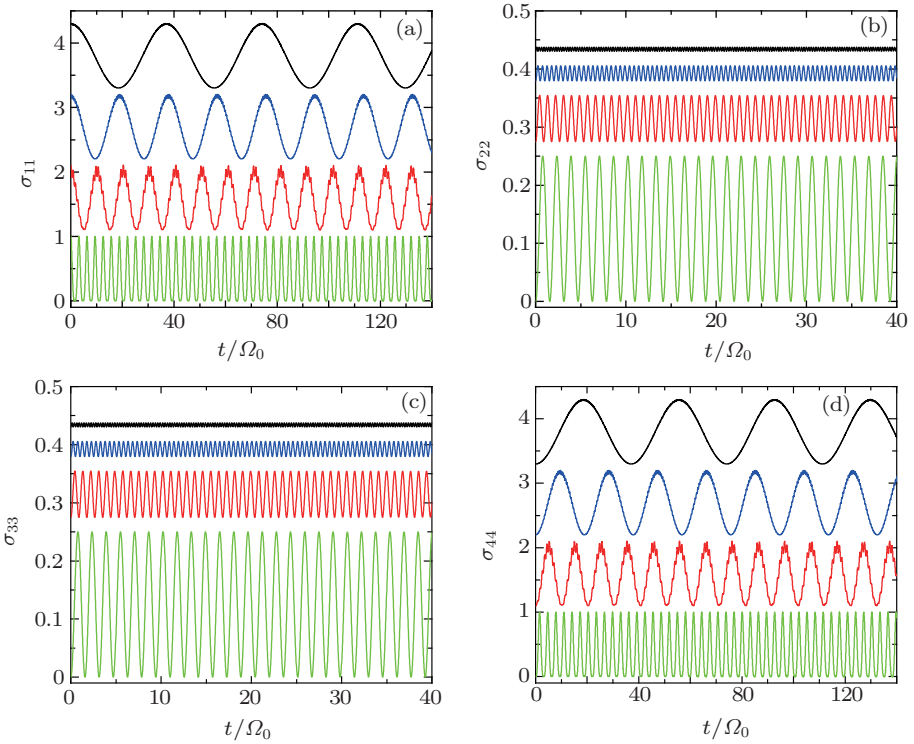


Fig. 3. (color online) Time-dependent electron occupation probability (a) σ_{11}, (b) σ_{22}, (c) σ_{33}, and (d) σ_{44} with the different Coulomb interactions. Each line from bottom to top in the figures corresponds to $U_1 = 0$, 20, 40, 80 respectively. Successive curves are offset for clarity.

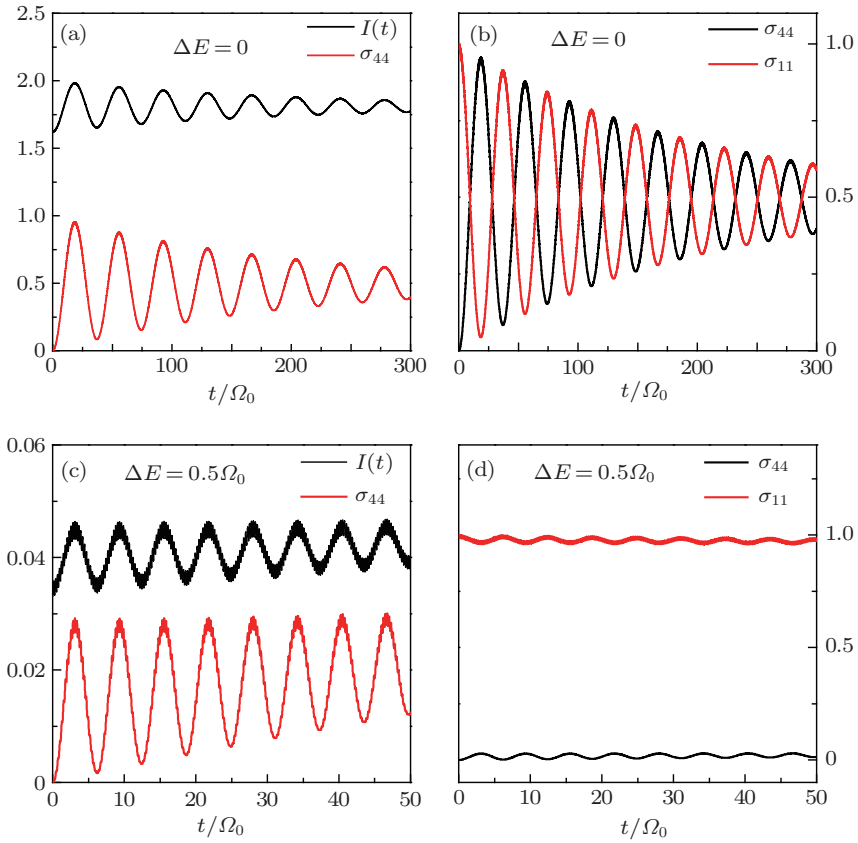


Fig. 4. (color online) The electron occupation probability σ_{11}, σ_{44}, and the QPC current $I(t)$ as a function of time. (a) and (b) the energy mismatch between the two dots $\Delta E = 0$; (c) and (d) the energy mismatch between the two dots $\Delta E = 0.5\Omega_0$. For clarity, the data for $I(t)$ in panel (c) are shifted.

5. The measurement of the quantum state of the CQDs via an rf-QPC circuit

In this paper we are quite interested in investigating the measurement of the quantum state via an rf-QPC circuit. Thus, we embed the whole CQDs and QPC system into the LC oscillator and get the numerical solution of the output voltage quadrature $V_{\rm out}^{\cos}(t)$ with no energy mismatch. We can safely ignore the other quadrature because it carries no information about qubits.[14] We keep $\varepsilon_{\rm in}=0.001$, which indicates a small-amplitude sinusoidal carrier signal and the coupling between the dots at a relatively large value $\Omega_0=10$ GHz that can be reached by tuning the gate voltage in an experiment.[19] Other parameters are set as $B=100$ MHz and $L=1$ μH giving a high quality factor of the unloaded circuit, $Q\approx 34$.[20–22] When we chose the resonance frequency $f=270$ MHz, which is roughly equal to the oscillation frequency of the QPC current, the oscillation of output voltage reflects that of the QPC current (see Fig. 5). Here, the damping $\gamma=Z_{\rm TL}/L\gg 1$ gives the circuit slaved to the quantum state. That is, $V_{\rm out}^{\cos}(t)$ is directly proportional to the quantum signal.[14] In addition, we find the wave shape is kept for about 15 ns. The scale of time is in accordance with that in Ref. [21]. After that time, the output voltage is chaotic, which means the output voltage cannot reflect the quantum information directly. The observer needs to invert the convolution to achieve the QPC current.

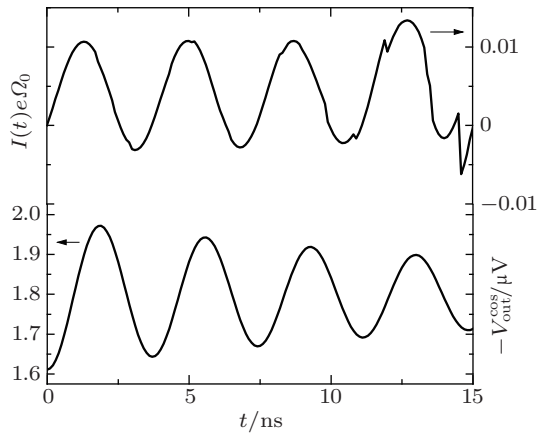


Fig. 5. The output voltage $-V_{\rm out}^{\cos}(t)$ and QPC current $I(t)$ as functions of time.

Furthermore, we are also interested in how the parameters of the circuit influence the output of the voltage signal. We make a shift in the resonance frequency f by adjusting the capacitance of the LC circuit. When $f=250$ MHz, the output voltage still reflects the oscillation of QPC current (see Fig. 6(a)). In contrast, an overdamping phenomenon exists when $f=300$ MHz (see Fig. 6(c)). The quality factor of detector QPC is $Q_{\rm d}\equiv\gamma_{\rm d}/\omega_0$ while the quality factor of the unloaded LC circuit is $Q\equiv\omega_0/\gamma$.[14] When the resonance frequency is relatively large, the quality factor of the loaded LC circuit $Q_T\equiv\left(Q^{-1}+Q_{\rm d}^{-1}\right)^{-1}$ depends mainly on $Q_{\rm d}$. Thus, we infer from Fig. 6 that $Q_{\rm d}$ shrinks sharply when the frequency of the LC circuit is larger than the QPC frequency. In addition, we find that increasing the bandwidth B helps keep the wave shape within the limit $\gamma<B<\omega_0$[14] (see Fig. 7). In experiments, it is also crucial to increase the single-shot spin readout fidelity.[24]

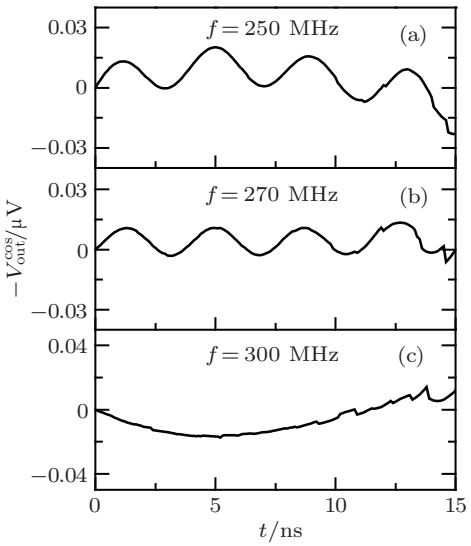


Fig. 6. The output voltage $-V_{\rm out}^{\cos}(t)$ as a function of time for (a) $f=250$ MHz, (b) $f=270$ MHz, and (c) $f=300$ MHz.

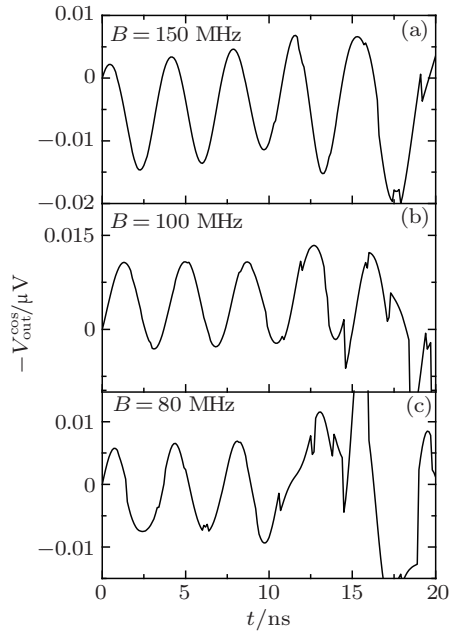


Fig. 7. The output voltage $-V_{\rm out}^{\cos}(t)$ as a function of time for the bandwidths (a) $B=150$ MHz, (b) $B=100$ MHz, and (c) $B=80$ MHz.

6. Summary

In this paper, we have derived the rate equations of the density matrix for CQDs monitored by a QPC detector and have applied the method developed by Gurvitz. Then, we put this model into an LC oscillator. Without the QPC detector,

we find that the electrons are inclined to stay in the localized states under the strong Coulomb interaction through numerical solution. With the QPC detector, the change of current $I(t)$ always reflects that of the probability that the electrons are in the right dot. The electrons remain in the initial localized state when energy displacement exists. For the circuit, the output voltage can reflect the change of QPC current by selecting the proper parameters. Increasing the resonance frequency could lead to overdamping output. Moreover, we can improve the bandwidth of the circuit for a better wave shape for output.

The output voltage we give is in the microvolt range. The output voltage can be amplified through cryogenic and room-temperature amplifier in experiments.[21] However, it is still challenging to perform such an experiment, especially for high bandwidth. We have so far considered the evolution of a reduced density matrix for the CQDs when all the measurement results are averaged.[5] To make contact with a single realization of the measurement records conditioned on a particular measurement realization, we would apply the realistic quantum trajectory theory[25] to this model in the next step.

References

[1] Masia F, Accanto N, Langbein W and Borri P 2012 *Phys. Rev. Lett.* **108** 087401

[2] Stemeroff N and de Sousa R 2011 *Phys. Rev. Lett.* **107** 197602

[3] Petta J R, Johnson A C, Yacoby A, Marcus C M, Hanson M P and Gossard A C 2005 *Phys. Rev. B* **72** 161301

[4] Nakamura Y, Pashkin Yu A and Tsai J S 1999 *Nature* **398** 786

[5] Goan H S, Milburn G J, Wiseman H M and Sun H B 2001 *Phys. Rev. B* **63** 125326

[6] Gurvitz S A 2005 *Phys. Rev. B* **72** 073303

[7] Gustavsson S, Leturcq R, Simovič B, Schleser R, Ihn T, Studerus P, Ensslin K, Driscoll D C and Gossard A C 2006 *Phys. Rev. Lett.* **96** 076605

[8] Gilad T and Gurvitz S A 2006 *Phys. Rev. Lett.* **97** 116806

[9] Fischer J, Coish W A, Bulaev D V and Loss D 2008 *Phys. Rev. B* **78** 155329

[10] Petersson K D, Petta J R, Lu H and Gossard A C 2010 *Phys. Rev. Lett.* **105** 246804

[11] Bennett C H 1995 *Phys. Today* **48**(10) 24

[12] Colless J I, Mahoney A C, Hornibrook J M, Doherty A C, Lu H, Gossard A C and Reilly D J 2013 *Phys. Rev. Lett.* **110** 046805

[13] Wang Q, Xie H Q, Jiao H J, Li Z J and Nie Y H 2012 *Chin. Phys. B* **21** 117310

[14] Oxtoby N P, Gambetta J and Wiseman H M 2008 *Phys. Rev. B* **77** 125304

[15] Clarke J 1989 *Proc. IEEE* **77** 1208

[16] Gurvitz S A and Prager Y S 1996 *Phys. Rev. B* **53** 15932

[17] Gurvitz S A 1997 *Phys. Rev. B* **56** 15215

[18] Wootters W K 1998 *Phys. Rev. Lett.* **80** 2245

[19] Gustavsson S, Studer M, Leturcq R, Ihn T, Ensslin K, Driscoll D C and Gossard A C 2007 *Phys. Rev. Lett.* **99** 206804

[20] Qin H and Williams D A 2006 *Appl. Phys. Lett.* **88** 203506

[21] Cassidy M C, Dzurak A S, Clark R G, Petersson K D, Farrer I, Ritchie D A and Smith C G 2007 *Appl. Phys. Lett.* **91** 222104

[22] Petersson K D, Smith C G, Anderson D, Atkinson P, Jones G A C and Ritchie D A 2010 *Nano Lett.* **10** 2789

[23] Reilly D J, Marcus C M, Hanson M P and Gossard A C 2007 *Appl. Phys. Lett.* **91** 162101

[24] Elzerman M, Hanson R, van Beveren L H W, Witkamp B, Vandersypen L M K and Kouwenhoven L P 2004 *Nature* **430** 431

[25] Oxtoby N P, Warszawski P, Wiseman H M, Sun H B and Polkinghorne R E S 2005 *Phys. Rev. B* **71** 165317